Chapter 2
Introduction to the Physics of Ultrasound

Pascal Laugier and Guillaume Haïat

Abstract From an acoustical point of view, bone is a complex medium as it is heterogeneous, anisotropic and viscoelastic. This chapter reviews the basic notions of physical acoustics which are necessary to tackle the problem of the ultrasonic propagation in bone, in the perspective of the application of quantitative ultrasound (QUS) techniques to bone characterization. The first section introduces the basic phenomena related to the field of medical ultrasound. Basic description of wave propagation is introduced. Mechanical bases are necessary to understand the elastodynamic nature of the interaction between bone and ultrasound. The physical determinants of the speed of sound of the different types of waves corresponding to the propagation in a liquid and in a solid are considered. The effects of boundary conditions (guided waves) are also detailed. The second section describes the physical interaction between an ultrasonic wave and bone tissue, by introducing reflection/refraction, attenuation and scattering phenomena.

Keywords Absorption · Anisotropy · Attenuation · Compression wave · Diffraction · Elastic modulus · Elastic solid · Group velocity · Guided wave · Impedance · Kramers Krönig · Lamb waves · Phase velocity · Poisson's ratio · Reflection · Refraction · Scattering · Shear wave · Snell's law · Speckle · Speed of sound · Stiffness · Strain · Stress · Young's modulus

2.1 Fundamentals of Ultrasound

In analogy to visible and ultraviolet light, the terms sound and ultrasound are used to describe the propagation of a mechanical perturbation in different frequency ranges. Ultrasound corresponds to a mechanical wave propagating at frequencies

P. Laugier (✉)
Université Pierre et Marie Curie, CNRS, Laboratoire d'Imagerie Parametrique,
15, rue de L'Ecole de Medecine, 75006 Paris, France
e-mail: pascal.laugier@upmc.fr

G. Haïat
CNRS, B2OA UMR 7052, 10, avenue de Verdun, 75010 Paris, France
e-mail: guillaume.haiat@univ-paris-est.fr

P. Laugier and G. Haïat (eds.), *Bone Quantitative Ultrasound*,
DOI 10.1007/978-94-007-0017-8_2,

above the range of human hearing (conventionally 20 kHz). Ultrasound and sound waves propagate in fluids (gases and liquids) and solids. The mechanical perturbation provokes tiny disturbances of the medium particles from their resting position. These disturbances induce a displacement of these particles and are transmitted step by step to other parts of the medium. The interaction between the particles can be schematically described using a mechanical spring analogy. In particular the wave propagation depends on the intrinsic elastic properties of the medium as well as on its mass density. For tiny perturbations (linear propagation regime), no mass is transported as the wave propagates from point to point: the medium as a whole remains stationary. In depth analysis of some aspects of non-linear propagation regimes will be provided in Chap. 15.

Perfect fluids (i.e. non viscous) support bulk compression waves only, which are characterized by density changes of the medium in which the particles oscillate in the longitudinal direction or the direction of wave propagation. Thus, bulk compression waves correspond to longitudinal waves. Moreover, bulk compression elastic waves can also propagate in solids. However, in solids unlike in fluids, a shearing strain produced at some point can be transmitted to adjacent layers by the strong binding between particles. This mechanism generates transverse waves also called bulk shear waves, for which the particle motion is perpendicular to the direction of propagation in the case of isotropic solids (refer to subsection 1.5.3 for the anisotropic case).

Biological soft tissues are viscoelastic solids, where both bulk compression and shear waves can propagate. However, typically, in soft tissues, ultrasound bulk shear waves are usually neglected because shear waves are highly attenuated at ultrasonic frequencies. However, in hard tissues like bone, both compression and shear waves must be considered.

The reader will find in what follows basic descriptions of elementary aspects of the physics of ultrasound. However, the aim of the authors only consists in introducing the basic description of fundamental phenomena involved in ultrasonic characterization of bone. Readers interested in deeper and more complete description of the acoustics of wave are referred to dedicated books [1–4].

2.1.1 Frequency–Period–Wavelength

As known from basic physics the characteristic variables describing the propagation of a monochromatic wave in time and space are frequency f or period T and wavelength λ given by:

$$\lambda = \frac{c}{f} = cT, \tag{2.1}$$

where c is the wave propagation velocity (also termed sound velocity or speed of sound). Typical diagnostic ultrasound devices employ frequencies in the range of 2–15 MHz. In contrast, due to the frequency dependence of ultrasound attenuation and to high attenuation values in bone, lower frequencies in the range of 250 kHz to

1.25 MHz are used in bone clinical devices, although higher frequencies have been tested experimentally, for example to investigate cancellous bone micro-structure [5] or to measure microelastic properties of cortical bone [6].

In cortical bone a typical sound velocity of $4000\,\mathrm{m}\cdot\mathrm{s}^{-1}$ results in a wavelength of 16 mm at 250 kHz and of 4 mm at 1.0 MHz. A representative value of sound velocity in cancellous bone of the human calcaneus is $1500\,\mathrm{m}\cdot\mathrm{s}^{-1}$ resulting in a wavelength of 3.1 mm at 500 kHz.

2.1.2 Phase Velocity–Group Velocity

Two fundamentally different sound velocities can be distinguished. Phase velocity corresponds to the propagation velocity of a given phase that is of a single frequency component of a periodic wave. A propagating medium is said to be dispersive if the phase velocity is a function of frequency or wavelength, which is the case for example in all attenuating media. This means that the different frequencies contained in the signal do not propagate at a constant velocity, which derive from the linearity and causality principles (see Chap. 12). Group velocity corresponds physically to the velocity at which energy or information is conveyed along the direction of propagation. In the case of a dispersive medium, the group velocity may differ from the phase velocity. It is important to be aware of velocity dispersion because it potentially affects the accuracy of speed of sound measurements [7–10]. Note that the attenuation coefficient and velocity dispersion are related through the Kramers-Krönig relationships [11, 12].

2.1.3 Notion of Stress

A stress is defined by a force per unit area applied to a given medium. Any stress applied to a solid can be expressed as a combination of pure compression and pure shear stresses [1]. If the solid is anisotropic the combination of compression and shear stresses can be described in terms of a stress matrix (also called stress tensor). In contrast, fluids only support pure compression stress, which is called pressure. A compression wave propagating in fluids or in isotropic solid media produces compressions and expansions, which causes pressure changes. The instantaneous value of the total pressure minus the ambient pressure is then called acoustic pressure or simply sound pressure. In contrast, shear wave causes shear stress.

We shall assume that the stress can be expressed in one-dimensional form and that therefore the waves are either purely longitudinal or purely transversal. This approach allows for a much simpler (but correct) description of the propagation phenomena. The description adopted for isotropic media can then be modified to take into account bone anisotropy (see for example Chap. 8).

2.1.4 Acoustic Impedance

During the propagation of an acoustic wave in a fluid, the particles of the medium are subject to displacements around their resting positions. The velocity of these displacements is called acoustic particle velocity and noted v. Thus, the particle velocity is the speed of motion of the particles due to the sound wave, it must be distinguished from the sound velocities defined in Sect. 1.2. For plane waves in a lossless medium (non-attenuating medium), the sound pressure p and particle velocity v are related to each other following :

$$p = \rho c v = Z v, \tag{2.2}$$

where ρ is the mass density of the medium at rest, and $Z = \rho \cdot c$ is called specific acoustic impedance.

2.1.5 Acoustic Intensity

The energy transported in an ultrasound wave is usually characterized by an acoustic intensity I defined as the energy transmitted per unit time (usually 1 s) and per unit area (usually $1\,\mathrm{cm}^2$) in the direction normal to the considered area. In the field of medical ultrasound, intensity is measured in $\mathrm{W}\cdot\mathrm{cm}^{-2}$. In the far field of an unfocused transducer where the wave front can be considered as a planar wave or at the focus of a focused transducer, the intensity of a monochromatic wave is related to the sound pressure as follows:

$$I = \frac{p^2}{2Z}. \tag{2.3}$$

2.1.6 Determinant of the Speed of Sound

In the linear propagation regime (tiny perturbation or small wave amplitude) speed of sound is a characteristic of the medium. It is independent from the wave amplitude and can be determined from the material and geometrical properties of the medium. To account for wave type, for example bulk compression, bulk shear, surface, or guided wave specific differences in c, the generalized concept of an effective elastic modulus M_e and an effective mass density ρ_e can be introduced [13]. The effective elastic modulus is related to elastic and geometrical characteristics of the medium, which determine the stiffness with respect to a given type of wave. The effective mass density is related to the inertia of the propagating medium. Following this concept c is expressed as:

$$c = \sqrt{\frac{M_e}{\rho_e}}. \tag{2.4}$$

A common correction in realistic systems is that speed of sound can also depend on the amplitude of the wave, leading to a nonlinear wave propagation (Chap. 15).

2.1.6.1 Case of a Fluid

In fluids, M_e is given by the adiabatic bulk modulus of elasticity K, the reciprocal of the adiabatic compressibility χ. The effective mass density ρ_e is the mass density of the fluid. The propagating waves are pure compression waves. K physically corresponds to the force opposing compression of the fluid. Compressibility is the relative change in volume when the pressure changes by one unit. A fluid model is generally adopted to describe waves at ultrasonic frequencies in soft tissue.

Of interest is the temperature dependence of c. Speed of sound in water is $1482\,\mathrm{m}\cdot\mathrm{s}^{-1}$ at 20°C. Between 20°C and 37°C it increases with a temperature coefficient of about $2.5\,\mathrm{m}\cdot\mathrm{s}^{-1}\cdot{}^{\circ}\mathrm{C}^{-1}$ [14]. As soft tissues are largely composed of water, it is not surprising that their speed of sound also increases with temperature. Fat is the exception. Speed of sound in fat decreases when temperature increases [15]. The observed temperature dependent decrease of c of trabecular bone marrow is also likely due to the influence of fat, an important component of bone marrow [16].

2.1.6.2 Case of an Infinite Isotropic Homogeneous Elastic Solids

For solids, M_e is given by a combination of the elastic properties. In general, this combination can be expressed using the different components of the elastic stiffness tensor (or matrix), noted c_{ij} and called stiffness coefficients. The stiffness coefficients are defined by the linear coefficients of proportionality between the different components of the stress and strain matrixes [17]. An isotropic homogeneous elastic solid can be equivalently described by:

- Two stiffness coefficients c_{11} and c_{12}
- The Lamé coefficients λ (bulk modulus, not to be confused with the wavelength) and μ (shear modulus)
- Two engineering constants such as E (Young's modulus) and ν (Poisson's ratio)

The Lamé coefficients (λ, μ) can be expressed as a function of the stiffness coefficients (c_{11}, c_{12}) or as a function of the engineering constants (E, ν). Similarly, the stiffness coefficients are related to the engineering constants. The full derivation of the wave propagation equation in anisotropic elastic solids is out of the scope of this chapter. Readers can find a comprehensive description in many classical textbooks, for example [1,2,17]. We only indicate in the following the principle of derivation of the wave propagation equation for the case of an isotropic linear elastic solid. Three equations are necessary to obtain the linear propagation equation in an isotropic solid. The first equation, corresponding to the constitutive law (Hooke's law) of the isotropic material considered, expresses the general relationship existing between

stress and strain in a perfectly elastic solid:

$$\sigma = \lambda \cdot tr(\varepsilon) + 2\mu\varepsilon, \tag{2.5}$$

where σ denotes the stress tensor, ε the strain tensor and tr(ε) is the trace of ε. The second equation corresponds to the equation of motion and is given by:

$$\rho \frac{\partial^2 u}{\partial t^2} = div(\sigma), \tag{2.6}$$

where ρ denotes the mass density of the solid, u denotes the elementary particle displacement vector and *div* the divergence operator ($div = \frac{\partial}{dx} + \frac{\partial}{dy} + \frac{\partial}{dz}$).

The last equation relates the strain tensor with the displacement field and is given by:

$$\varepsilon = \frac{1}{2}(grad(u) +^T grad(u)), \tag{2.7}$$

where grad indicates the gradient tensor and $^{\mathrm{T}}$ indicates the transpose operation. By combining Eqs. 2.5–2.7 and considering respectively the case where the particle displacement is parallel and perpendicular to the direction of propagation, the wave propagation equations corresponding to the case of a longitudinal and shear wave mode are obtained and are given respectively by:

$$\rho \frac{\partial^2 u}{\partial t^2} = (\lambda + 2\mu) \cdot \Delta u \text{ and } \rho \frac{\partial^2 u}{\partial t^2} = \mu \cdot \Delta u \tag{2.8}$$

where Δ denotes the Laplacian operator: $\Delta = \frac{\partial^2}{dx^2} + \frac{\partial^2}{dy^2} + \frac{\partial^2}{dz^2}$.

In summary, in an infinite isotropic homogeneous solid body, in which the propagating wave does not interact with the boundary of the medium, the longitudinal and shear (transversal) propagation velocity c_l and $c_s$are given by [1]:

$$c_l = \sqrt{\frac{\lambda + 2\mu}{\rho}} = \sqrt{\frac{c_{11}}{\rho}} = \sqrt{\frac{E(1-\nu)}{\rho(1+\nu)(1-2\nu)}} \tag{2.9}$$

and

$$c_s = \sqrt{\frac{\mu}{\rho}} = \sqrt{\frac{c_{11} - c_{12}}{2\rho}} = \sqrt{\frac{E}{\rho(1+\nu)}} \tag{2.10}$$

2.1.6.3 Infinite Anisotropic Homogeneous Elastic Solids

In homogeneous anisotropic media, the elastic properties depend on the direction of propagation of the acoustical wave. For example, in crystalline materials, the elastic properties (and thus the sound velocities) depend on the orientation of the crystalline directions relative to the direction of propagation. In this case, M_e

depends on the direction of propagation, wave polarization (the direction of particle displacement with respect to propagation direction) and crystal class of symmetry. For an arbitrary direction in a crystal, three wave types can generally propagate: one quasi-longitudinal and two quasi-transverse waves. However, there are special directions called symmetry axes along which pure longitudinal or shear waves propagate. Details of the relationships between sound velocity and elastic coefficients for infinite anisotropic elastic solids are beyond the scope of this chapter and can be found in reference books on elastic waves in solids [1–3].

For cortical bone the general degree of anisotropy is that of orthotropic material symmetry [18], which is characterized by nine independent stiffness coefficients. A simplified model of a transverse isotropic elastic solid medium, which reduces the number of independent coefficients of the stiffness matrix to five, has also been considered [19–23]. The directional dependence of engineering elastic moduli such as E or σ can then be derived from the stiffness coefficients. These assumptions about bone symmetry were used successfully in studying in vitro ultrasound propagation along the various symmetry axes of cortical bone specimens [18, 21, 24, 25].

2.1.6.4 Finite Homogeneous Elastic Solids

Equations 2.9 and 2.10 were introduced for unbounded media assuming that the wavelength λ is much smaller than the smallest sample dimension. In the opposite case (e.g., when the propagation medium is thin compared to λ), multiple reflections, mode conversions and interferences of longitudinal and shear waves from the sample boundaries occur. These phenomena create a wave guide character of the sound propagation within boundaries of the considered medium. In this case, sound perturbations can be represented as superposition of resonant guided wave modes (so-called eigen modes).

Guided wave modes which exist in plates are known as Lamb waves, which are complex waves traveling through the entire plate. Different families of Lamb wave modes can be distinguished including symmetrical modes (in-phase displacements of opposite plate surfaces) and asymmetrical or flexural modes (anti-phase displacements of opposite plate surfaces), as shown in Fig. 2.1.

Guided wave modes have been described for rods [3] as well as for tubes [26]. Guided wave modes are always dispersive, which means that their phase velocities are function of the wavelength (or frequency) and of the layer thickness.

Fig. 2.1 Illustration of symmetrical and asymmetrical guided wave modes propagating through the entire thickness of a plate

In addition, phase velocity is also function of the elastic properties and density of the medium [27].

The wave guide character of the sound propagation has been evidenced for cortical bone in the 0.25–2 MHz frequency range. In this case, cortical bone can be modeled as a plate-like (2-D description) or a tube-like (3-D description) layered medium [27, 28].

A particular case of guided wave is the extensional or bar wave in a thin rod, a configuration which has been used to measure the properties of cortical bone. Under the assumption that the cross-sectional dimensions of the rod (in the case of a cylindrical rod, its diameter) are much smaller than λ, only a longitudinal stress component can be considered along the propagation direction of the rod. In this case, the speed of sound c is given by [13]:

$$c = \sqrt{\frac{E}{\rho}} \Leftrightarrow E = \rho\, c^2 \tag{2.11}$$

For in vivo measurements purposes, guided waves in cortical bone can be excited from the surrounding soft tissues using an incident beam at a specific angle [28]. If a wave is guided by the bone cortex with a phase velocity greater than that of the compression wave of the surrounding soft tissues, the energy propagating in the bone cortex can leak into the soft tissue. Thus, power is continuously radiated into the soft tissues, the guided wave mode can be detected and its velocity measured with sensors placed at its surface. A comprehensive review of guided waves used to investigate cortical bone is given in Chap. 7.

2.1.6.5 Inhomogeneous Elastic Solids

In the sections above, the sound wave propagation was restricted to homogeneous elastic solids. However, bone is highly heterogeneous at different scales, and can be described by a composite and poroelastic material. The derivation of M_e for composite or poroelastic materials may be rather complex and requires cumbersome theoretical developments. Moreover, due to the important difference in porosity and structure between cortical and trabecular bone, the analysis of ultrasound propagation may require different theoretical frameworks for these two types of bone structures.

As the medium is no longer homogeneous but rather a mixture of several components such as collagen fibers, hydroxyapatite crystals, water, non-collagen substance and marrow, which are all characterized by different elastic coefficients, it remains difficult to simply determine M_e. Replacing the actual material by a homogenized material is the best we can expect. M_e can then be determined assuming that λ is much larger than d, where d is the characteristic size of the structural heterogeneities such as, for example, osteons, Haversian canals, osteocytes, lacunae, apatite crystals and collagen fibers. At the scale of the wavelength, the medium can then be considered homogeneous and therefore Eqs. 2.9 and 2.10 can be applied using the

homogenized stiffness coefficients. The effective elastic modulus and the effective mass density can be derived from experiments or theoretical models. Different multiscale homogenization approaches [20, 29–32] have been developed to determine a homogenized value for M_e, which is the only way to practically estimate the material properties at the scale of λ.

The porosity of human cortical bone is rather low and the pore size ($\sim$50 to 100 µm) is smaller than typical wavelengths (>1 mm). Therefore, the aforementioned homogenization theories can be applied and cortical bone can be modeled as a mono-phase homogeneous medium (rather than a two-phase medium) in regard to the ultrasonic propagation. Therefore, ultrasound propagation at diagnostic frequencies (around 1 MHz) in cortical bone can be described at first approximation by the propagation in an anisotropic homogeneous medium (see Chap. 13).

In contrast, such an assumption is not valid for cancellous bone where porosity values are rather high. The pore size ($\sim$500 to 1000 µm) is comparable to the wavelength (1.5 mm at 500 kHz). The elasticity of such a poroelastic structure then intrinsically depends on the structure of the bone. Several theoretical concepts considering poroelasticity such as Biot's theory [33–39] and Schoenberg's theory for multilayered media [40–44] have been applied to describe ultrasound propagation in cancellous bone. These models will be detailed in Chap. 5.

2.2 Tissue Interaction

2.2.1 Specular Reflection and Refraction

As known from basic physics, reflection and refraction occur at the boundary between two media with different characteristic acoustic impedances or different speeds of sound. If the surface is smooth compared to the wavelength, specular reflections occur whereas for rough surfaces, reflections are diffuse [45]. Specular reflection forms the basis of pulse-echo ultrasonic imaging (echography) and contributes to image formation displaying organ boundaries. It is convenient to distinguish fluid–fluid interfaces such as the discontinuity between two soft tissues, which is the typical model for diagnostic clinical ultrasound, and fluid-solid interfaces, which represent more realistically the boundary between soft tissue and cortical bone. The interaction between ultrasound and cancellous bone is more complicated. It can best be described by scattering phenomena, which will be discussed in Sect. 2.3. In what follows, we shall assume that the incident wave is a plane wave in the fluid for the sake of simplicity.[1]

[1] Any kind of wave may be decomposed in a sum of planar waves.

2.2.1.1 Fluid–Fluid Interface

If a plane wave impinges on a smooth plane interface (i.e. under the assumption of specular reflection), a reflected and a transmitted wave will be generated (see Fig. 2.2a). As only longitudinal waves can exist in a fluid, the refracted and reflected waves are also longitudinal. According to Snell's law, (i) the reflection angle θ_1 is equal to the angle of the incident wave and (ii) the transmitted wave is refracted away from the direction of the incident wave θ_1 at a refraction angle θ_2 given by:

$$\frac{\sin\theta_2}{c_2} = \frac{\sin\theta_1}{c_1}, \tag{2.12}$$

where and c_1 and c_2 are the sound velocities of the first and second medium.

For normal incidence ($\theta_1 = 0^\circ$), the reflected and transmitted waves are also normal to the interface. The ratio of the reflected to the incident acoustic pressure amplitude is called amplitude reflection coefficient r. The ratio of the transmitted to the incident acoustic amplitude is called amplitude transmission coefficient t. Coefficients t and r are given by:

$$r = \frac{Z_1 - Z_2}{Z_1 + Z_2} \quad t = \frac{2Z_2}{Z_1 + Z_2}. \tag{2.13}$$

Similarly intensity reflection (R) and transmission coefficients (T) are defined by the ratio of the reflected to the incident acoustic intensity and the ratio of the transmitted to the incident acoustic amplitude, respectively:

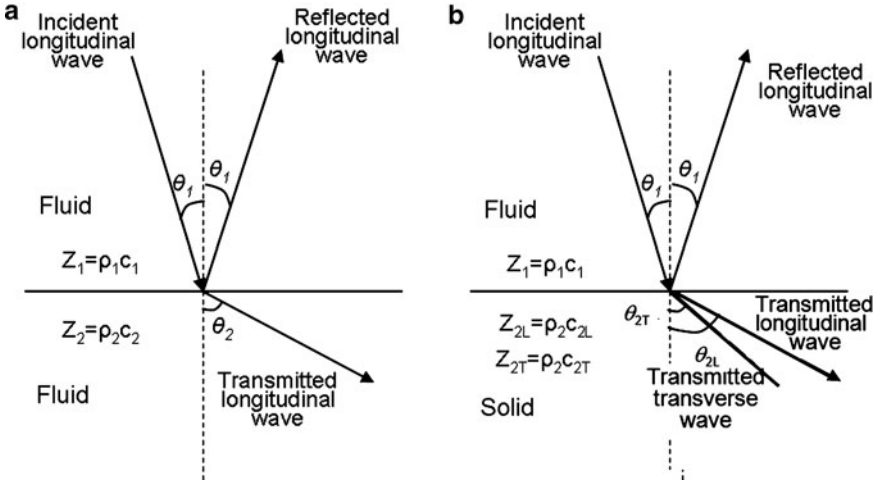

Fig. 2.2 Reflection and refraction at the boundary (**a**) between two fluid media and (**b**) between a fluid and a solid medium

Table 2.1 Typical values for sound velocity, characteristic acoustic impedance, and attenuation (see next section) in different biological tissues for temperatures in the range between 20°C and 37°C. These values are only indicative of the order of magnitude, due to dramatic biological variability

Tissue	Ultrasound propagation velocity c $(m \cdot s^{-1})$	Characteristic acoustic impedance Z $(kg \cdot s^{-1} \cdot m^{-2})$	Slope of the attenuation coefficient $(dB \cdot cm^{-1} \cdot MHz^{-1})$
Water (20°C)	1480	1.48×10^6	[a]
Cancellous bone	1450–1800	$1.54 \times 10^6 - 2.2 \times 10^6$	10–40
Cortical bone	3000–4000	$4 \times 10^6 - 8 \times 10^6$	1–10
Fat	1450	1.38×10^6	0.8
Muscle	1550–1630	$1.65 \times 10^6 - 1.74 \times 10^6$	0.5–1.5
Skin	1600	1.7×10^6	2–4

[a] The attenuation in water exhibits a quadratic variation with frequency f. Its attenuation coefficient in $dB \cdot cm^{-1}$ is $\alpha(f) = 0.002f^2$

$$R = \left(\frac{Z_1 - Z_2}{Z_1 + Z_2}\right)^2 \quad T = \frac{4Z_1Z_2}{(Z_1 + Z_2)^2}. \tag{2.14}$$

where Z_1 and Z_2 are the characteristic acoustic impedances of the first and second medium for longitudinal waves, respectively. One can verify that $T + R = 1$, which corresponds to the conservation of energy equation (in the lossless case). The amount of energy in the reflected wave depends on the impedance discontinuity of the two media. The greater the difference, the greater is the reflected energy.

Table 2.1 shows the different values of sound velocity, of acoustic impedance, and of the slope of the attenuation coefficient as a function of frequency for selected tissues playing a part in bone QUS evaluation. As can be seen, for soft tissues Z differs only slightly from that of water. In case of small impedance discontinuities (e.g., such as between two soft tissues), the reflected beam typically carries less than 1% of the incident energy and 99% or more of the incident energy is transmitted through the interface. Because of relatively small velocity changes in various soft tissues, refraction is generally not a serious problem.

2.2.1.2 Fluid–Solid Interface

In the case where the second medium is a solid such as cortical bone, Eq. 2.13 represents the ideal case for normal incidence and serves as guidelines to determine the reflected and transmitted energies. When ultrasound strikes a cortical bone interface at normal incidence, approximately 25–50% of the incident energy is transferred to the reflected wave and only 75–50% to the refracted longitudinal wave.

For oblique incidence the refracted longitudinal plane wave in the solid is partially converted into a shear wave, and two refracted beams exist, as shown in

Fig. 2.2b. For oblique incidence Snell's law must be generalized to [1]:

$$\frac{\sin(\theta_1)}{c_1} = \frac{\sin(\theta_{2L})}{c_{2L}} = \frac{\sin(\theta_{2T})}{c_{2T}}, \tag{2.15}$$

where subscripts 2L and 2T refer respectively to the refracted longitudinal and shear waves in the solid medium (e.g., bone). As longitudinal waves in solids propagate most of the time with a greater sound speed than in fluids, the refraction angle θ_{2L} is larger than the angle of incidence θ_I. When θ_I is higher than a certain value θ_c, total internal reflection occurs and the longitudinal wave is no longer transmitted into the solid. The refracted wave is termed evanescent as it travels parallel to the interface and decays exponentially from the boundary. The corresponding incident angle θ_c is termed the first critical angle and is given by:

$$\sin(\theta_c) = \frac{c_1}{c_{2L}}. \tag{2.16}$$

The value of longitudinal wave velocity in cortical bone stands in the range 3500–4200 $\mathrm{m \cdot s^{-1}}$ (see Chap. 13), which gives typical values of θ_c between 20° and 25°.

If the velocity of the shear wave in the solid is also greater than the velocity of the longitudinal wave in the fluid then analogously there is a second critical angle at which the shear refracted beam propagates along the surface. Actually, the propagation of sound waves in solids is even more complicated and several critical angles may exist [1, 17]. The measurement of critical angles is the basis of ultrasound critical-angle reflectometry (UCR), which has been used to characterize bone in vitro as well as in vivo [46–48]. In UCR, the sound velocities of the longitudinal and the shear waves in cortical bone can directly be determined from θ_c according to Snell's law if the speed of sound of the surrounding fluid (or soft tissue) is known precisely.

2.2.2 Attenuation

Two main mechanisms contribute to ultrasound attenuation: absorption and scattering. Different mechanisms are responsible for absorption phenomena (thermal conductance effects, chemical effects, viscous effects, non linearity ...). So far, the phenomena responsible for ultrasound absorption in biological tissues have not been completely understood. In liquids (respectively homogeneous solids), the viscous (respectively viscoelastic) forces between neighboring particles moving with different velocities are major sources of acoustic wave absorption. For example, viscous losses may explain sound wave absorption in water where attenuation varies with the square of the frequency. However, this model of viscosity (quadratic dependence of the attenuation coefficient versus frequency) does not explain experimental mea-

surements of absorption in soft biological tissues as well as in bone in the diagnostic frequency range.

Other models hypothesized that a significant fraction of the absorption of longitudinal waves in soft tissues involves a spectrum of relaxation mechanisms at the macromolecular scale of proteins [49] or potentially thermal transport phenomena arising from temperature gradients in the medium [50]. In the frequency range where characteristic relaxation times are close to the wave time period, a quasi-linear variation of the attenuation coefficient with frequency can be observed.

Attenuation differs substantially between fluid-like soft tissues and porous media such as bone, in which (i) viscous friction effects due to the relative motion of marrow and solid frame, (ii) scattering of the ultrasonic wave by bone heterogeneity and (iii) longitudinal to shear mode conversion contribute significantly. The mechanisms of scattering will be presented in the next section. Acoustic attenuation in cancellous bone is usually almost one order of magnitude higher than in cortical bone. This is likely due to the large bone surface-to-volume ratio, which reinforces scattering, mode conversion and viscous friction. Recent studies suggest that loss mechanisms such as mode conversion, that is the transformation of longitudinal waves into shear waves (and subsequent absorption of these shear waves) occurring at the surface of the scattering particles, may be a significant contributor to the overall attenuation in bone in the diagnostic frequency range [51, 52].

Further important factors that contribute to the total wave intensity attenuation as it propagates through a complex medium such as a limb composed of several layers of different media (surrounding soft tissues, bone, marrow) are diffraction, reflection and refraction. Due to diffraction phenomena, the acoustic beam emitted from a planar (unfocused) transducer will increase its diameter as the wave propagates and the intensity will decrease with increasing distance from the source. Reflection and refraction losses at tissue interfaces according to Eq. 2.13 depend on the impedance mismatch at the interfaces. In general, overall ultrasound attenuation is characterized by the following exponential decrease of the pressure amplitude p and of the amplitude of the acoustic intensity I with the traveling distance z:

$$p = p_0 e^{-\alpha z} \text{ and } I = I_0 e^{-2\alpha z} \tag{2.17}$$

where p_0 and I_0 are the pressure and intensity at $z = 0$, respectively. The quantity α (expressed in cm^{-1}) is the pressure frequency-dependent attenuation coefficient. The factor 2 in the exponential term of the intensity equation results from transforming pressure into intensity, as intensity is proportional to the square of pressure. In biomedical ultrasonics, the commonly used units for α and for its slope when plotted versus frequency are $\text{dB} \cdot \text{cm}^{-1}$ and $\text{dB} \cdot \text{cm}^{-1} \cdot \text{MHz}^{-1}$, respectively. The unit conversion cm^{-1} to $\text{dB} \cdot \text{cm}^{-1}$ writes [53]:

$$\alpha[dB \cdot cm^{-1}] = \frac{1}{z} \cdot 10 \ln \frac{I_0}{I} = 8.686 \alpha[cm^{-1}] \tag{2.18}$$

Some authors use α as the intensity frequency-dependent attenuation coefficient ($I = I_0 e^{-\alpha z}$). Then, the conversion to dB results in $\alpha[\mathrm{dB \cdot cm^{-1}}] = 4.343\alpha[\mathrm{cm^{-1}}]$.

2.2.3 Tissue Penetration

It has been shown experimentally that ultrasound attenuation in biological tissues varies approximately linearly with frequency [54]. The linear dependency has been documented for soft tissues over a broad frequency range from 1 to 50 MHz and also for cancellous bone in a limited frequency range of 0.2–2 MHz [55–59]. Since attenuation in tissues increases with frequency, the price paid for using shorter wavelengths (that is for improving spatial resolution) is an increase in attenuation, which limits the possible penetration depth due to the sensitivity of the sensor. For most soft tissues, values of the slope of the attenuation coefficient versus frequency are approximately comprised in the range $0.5–1.0\,\mathrm{dB \cdot cm^{-1} \cdot MHz^{-1}}$ (see Table 2.1). In bone, the slope of the attenuation coefficient is one or two orders of magnitude higher than in soft tissues. Hence, lower frequencies (around 0.5–1 MHz) are commonly used for skeletal investigations.

2.2.4 Scattering

Scattering phenomena result from the interaction between a primary ultrasonic wave and the boundaries of particles (inhomogeneities) if their physical properties such as density or elasticity are different from those of the surrounding medium. In this case, the oscillatory movement of the scatterer is different from that of the surrounding medium, which leads to the emission of a secondary wave denoted scattered wave.

The scattering regime of a single particle depends on the ratio between its dimension and λ. If λ is much smaller than the size of the heterogeneity, specular reflection obeying the usual laws of reflection occurs (see Eq. 2.13). In contrast, a scattered wave is created if the dimensions of the heterogeneities are comparable to or lower than the wavelength. The scattering problem of light and sound by small scatterers was first solved by Lord Rayleigh [60] and is therefore called Rayleigh scattering. For scatterers much smaller than the wavelength, the intensity of the scattered waves is proportional to the fourth power of the frequency of the incident wave. It is also proportional to the sixth power of the size of the scatterers, i.e., to the square of its volume [61]. The case of scatterers with larger sizes or sizes comparable to the wavelength involves more complicated calculations [61].

The scattered intensity from soft tissue is generally considerably smaller than the specularly reflected intensity from organ boundaries. However, similar to specular reflection, such scattering events are of primary importance for image formation and for assessing micro-structural properties of the medium such as scatterer size of scatterer number density. In ultrasound images of soft tissues, scattering causes the grainy aspect or echostructure, also denoted speckle.

In soft tissue, the density and compressibility of scatterers are close to those of the surrounding medium. Thus the contribution of scattering to overall attenuation is relatively small. At low MHz frequencies, attenuation by scattering in soft tissue is typically 10–15% of the total attenuation [62]. In contrast, scattering is likely to be an important attenuation mechanism in bone. Although scattering from bone has received less attention than attenuation and sound velocity, its study is important because it may explain mechanisms responsible for attenuation [51] and for velocity dispersion [63]. Ultrasonic scattering predominantly occurs in cancellous bone in comparison to cortical bone. Cancellous bone can be considered as a highly inhomogeneous scattering medium: a soft tissue-like medium, i.e. bone marrow, containing a solid matrix, i.e. mineralized collagen of interconnected trabecular elements with a mean thickness ranging from 50 to 150 µm. Trabeculae are likely candidates for scattering sites due to the high contrast in acoustic properties between mineralized tissue and marrow [64]. Various scattering models for trabecular bone have been proposed and will be extensively presented in Chap. 6.

References

1. D. Royer and E. Dieulesaint, *Elastic Waves in Solids I* (Springer, New York, 2000).
2. B. A. Auld, *Acoustic Fields and Waves in Solids* (Krieger Pub Co, New York, 1990).
3. J. D. Achenbach, *Wave Propagation in Elastic Solids* (Elsevier, Amsterdam, 1973).
4. S. Temkin, *Elements of Acoustics* (John Wiley & Sons Inc, New York, 1981).
5. M. A. Hakulinen, J. S. Day, J. Toyras, H. Weinans, and J. S. Jurvelin, "Ultrasonic characterization of human trabecular bone microstructure," Phys Med Biol. **51**(6), 1633–1648 (2006).
6. K. Raum, "Microelastic imaging of bone," IEEE Trans Ultrason Ferroelectr Freq Control **55**(7), 1417–1431 (2008).
7. G. Haïat, F. Padilla, R. Barkmann, S. Dencks, U. Moser, C.-C. Glüer, and P. Laugier, "Optimal prediction of bone mineral density with ultrasonic measurements in excised human femur," Calcif Tissue Int **77**(3) (2005).
8. G. Haïat, F. Padilla, R. O. Cleveland, and P. Laugier, "Effects of frequency-dependent attenuation and velocity dispersion on in vitro ultrasound velocity measurements in intact human femur specimens," IEEE Trans Ultrason Ferroelectr Freq Control **53**(1), 39–51 (2006).
9. K. A. Wear, "The effects of frequency-dependant attenuation and dispersion on sound speed measurements: applications in human trabecular bone," IEEE Trans Ultrason Ferroelectr Freq Control **47**(1), 265–273 (2000).
10. K. A. Wear, "A numerical method to predict the effects of frequency-dependent attenuation and dispersion on speed of sound estimates in cancellous bone," J Acoust Soc Am **109**(3), 1213–1218 (2001).
11. M. O'Donnell, E. T. Jaynes, and J. G. Miller, "General relationships between ultrasonic attenuation and dispersion," J Acoust Soc Am **63**(6) (1978).
12. M. O'Donnell, E. T. Jaynes, and J. G. Miller, "Kramers-Kronig relationship between ultrasonic attenuation and phase velocity," J Acoust Soc Am **69**(3), 696–701 (1981).
13. V. Shutilov, *Fundamental Physics of Ultrasound* (Gordon and Breach, New York, 1988).
14. N. Bilaniuk and G. S. K. Wong, "Speed of sound in pure wateras a function of temperature," J Acoust Soc Am **93**(3), 1609–1612 (1993).
15. S. A. Goss, R. L. Johnston, and F. Dunn, "Comprehensive compilation of empirical ultrasonic properties of mammalian tissues," J Acoust Soc Am **64**(2), 423–457 (1978).
16. P. H. Nicholson and M. L. Bouxsein, "Effect of temperature on ultrasonic properties of the calcaneus in situ," Osteoporos Int **13**(11), 888–892 (2002).

17. G. S. Kino, *Acoustic Waves: Devised Imaging and Analog Signal* (Prentice Hall, Englewood Cliffs, 1987).
18. R. B. Ashman, S. C. Cowin, W. C. Van Buskirk, and J. C. Rice, "A continuous wave technique for the mesurement of the elastic properties of cortical bone," J Biomech **17**, 349–361 (1984).
19. J. L. Katz, "Anisotropy of Young's modulus of bone," Nature **283**, 106–107 (1980).
20. P. J. Arnoux, J. Bonnoit, P. Chabrand, M. Jean, and M. Pithioux, "Numerical damage models using a structural approach: application in bones and ligaments," Eur Phys J Appl Phys **17**, 65–73 (2002).
21. H. S. Yoon and J. L. Katz, "Ultrasonic wave propagation inhuman cortical bone - II. Measurements of elastic properties and microhardness," J Biomech **9**, 459–464 (1976).
22. G. Haiat, S. Naili, Q. Grimal, M. Talmant, C. Desceliers, and C. Soize, "Influence of a gradient of material properties on ultrasonic wave propagation in cortical bone: application to axial transmission," J Acoust Soc Am. **125**(6), 4043–4052 (2009).
23. E. Bossy, M. Talmant, and P. Laugier, "Three-dimensional simulations of ultrasonic axial transmission velocity measurement on cortical bone models," J Acoust Soc Am **115**(5 Pt 1), 2314–2324 (2004).
24. S. B. Lang, "Ultrasonic method for measuring elastic coefficients of bone and results on fresh and dried bovine bones," IEEE T Bio-med Eng **BME-17**(2), 101–105 (1970).
25. L. Serpe and J. Y. Rho, "The nonlinear transition period of broadband ultrasonic attenuation as bone density varies," J Biomech **29**, 963–966 (1996).
26. D. Gazis, "Three-dimensional investigation of the propagation of waves in hollow circular cylinders.II. Numerical Results," J Acoust Soc Am **31**(5), 573–578 (1959).
27. I. Viktorov, *Rayleigh and Lamb Waves* (Plenum, New York, 1967).
28. P. Moilanen, "Ultrasonic guided waves in bone," IEEE Trans Ultrason Ferroelectr Freq Control **55**(6), 1277–1286 (2008).
29. C. Hellmich and F. J. Ulm, "Micromechanical model for ultrastructural stiffness of mineralized tissues," J Eng Mech **128**(8), 898–908 (2002).
30. J. M. Crolet, B. Aoubiza, and A. Meunier, "Compact bone: numerical simulation of mechanical characteristics," J Biomech **26**(6), 677–687 (1993).
31. B. Aoubiza, J. M. Crolet, and A. Meunier, "On the mechanical characterization of compact bone structure using the homogenization theory," J Biomech **29**(12), 1539–1547 (1996).
32. C. Hellmisch and F. J. Ulm, "Micromechanical Model for Ultrastructural Stiffness of Mineralized Tissues," J Eng Mech **128**(8), 898–908 (2002).
33. A. Hosokawa, "Simulation of ultrasound propagation through bovine cancellous bone using elastic and Biot's finite-difference time-domain methods," J Acoust Soc Am **118**(3 Pt 1), 1782–1789 (2005).
34. A. Hosokawa and T. Otani, "Acoustic anisotropy in bovine cancellous bone," J Acoust Soc Am **103**(5), 2718–2722 (1998).
35. Z. E. Fellah, J. Y. Chapelon, S. Berger, W. Lauriks, and C. Depollier, "Ultrasonic wave propagation in human cancellous bone: application of Biot theory," J Acoust Soc Am **116**(1), 61–73 (2004).
36. E. R. Hughes, T. G. Leighton, G. W. Petley, P. R. White, and R. C. Chivers, "Estimation of critical and viscous frequencies for Biot theory in cancellous bone," Ultrasonics **41**(5), 365–368 (2003).
37. K. I. Lee, H. S. Roh, and S. W. Yoon, "Correlations between acoustic properties and bone density in bovine cancellous bone from 0.5 to 2 MHz," J Acoust Soc Am **113**(5), 2933–2938 (2003).
38. K. A. Wear, A. Laib, A. P. Stuber, and J. C. Reynolds, "Comparison of measurements of phase velocity in human calcaneus to Biot theory," J Acoust Soc Am **117**(5), 3319–3324 (2005).
39. J. L. Williams, "Ultrasonic wave propagation in cancellous and cortical bone: Prediction of experimental results by Biot's theory," J Acoust Soc Am **91**(2), 1106–1112 (1992).
40. E. R. Hubbuck, T. G. Leighton, P. R. White, and G. W. Petley, "A stratified model for ultrasonic propagation in cancellous bone," presented at the Joint meeting of the 16th International Congress on Acoustics and the 135th Meeting of the Acoustical Society of America, Seattle, Washington, June 20–26, 1998.

41. E. R. Hughes, T. G. Leighton, G. W. Petley, and P. R. White, "Ultrasonic propagation in cancellous bone: a new stratified model," Ultrasound Med Biol. **25**(5), 811–821 (1999).
42. W. Lin, Y. X. Qin, and C. Rubin, "Ultrasonic wave propagation in trabecular bone predicted by the stratified model," Ann Biomed Eng **29**(9), 781–790 (2001).
43. F. Padilla and P. Laugier, "Phase and group velocities of fast and slow compressional waves in trabecular bone," J Acoust Soc Am **108**(4), 1949–1952 (2000).
44. K. A. Wear, "A stratified model to predict dispersion in trabecular bone," IEEE Trans Ultrason Ferroelectr Freq Control **48**(4), 1079–1083 (2001).
45. A. Ishimaru, *Wave Propagation and Scattering in Random Media* (Wiley, NewYork, 1999).
46. P. P. Antich, J. A. Anderson, R. B. Ashman, J. E. Dowdey, J. Gonzales, R. C. Murry, J. E. Zerwekh, and C. Y. Pak, "Measurement of mechanical properties of bone material in vitro by ultrasound reflection: methodology and comparison with ultrasound transmission," J Bone Miner Res **6**(4), 417–426 (1991).
47. P. P. Antich, C. Y. C. Pak, J. Gonzales, J. A. Anderson, R. B. Ashman, K. Sakhaee, and C. Rubin, "Measurement of intrinsic bone quality in vivo by reflection ultrasound: correction of impaired quality with slow-release sodium fluoride and calcium citrate," J Bone Miner Res **8**(3), 301–311 (1993).
48. S. S. Mehta, P. P. Antich, M. M. Daphtary, D. G. Bronson, and E. Richer, "Bone material ultrasound velocity is predictive of whole bone strength," Ultrasound Med Biol **27**(6), 861–867 (2001).
49. J. C. Bamber, *Physical Principles of Medical Ultrasonics* (John Wiley & Sons, Chichester, UK, 1986).
50. K. S. Peat and R. Kirby, "Acoustic wave motion along a narrow cylindrical duct in the presence of an axial mean flow and temperature gradient," J Acoust Soc Am **107**(4), 1859–1867 (2000).
51. E. Bossy, F. Padilla, F. Peyrin, and P. Laugier, "Three-dimensional simulation of ultrasound propagation through trabecular bone structures measured by synchrotron microtomography," Phys Med Biol **50**(23), 5545–5556 (2005).
52. K. A. Wear, "Mechanisms for attenuation in cancellous-bone-mimicking phantoms.," IEEE Trans Ultrason Ferroelectr Freq Control **55**(11), 2418–2425 (2008).
53. T. L. Szabo, *Diagnostic Ultrasound*, Academic press series on biomedical engineering (Elsevier Academic Press, London, UK, 2004).
54. K. T. Dussik and D. J. Fritch, "Determination of sound attenuation and sound velocity in the structure constituting the joints, and of the ultrasonic field distribution with the joints of living tissues and anatomical preparations, both in normal and pathological conditions" (1956).
55. S. Chaffaï, F. Padilla, G. Berger, and P. Laugier, "In vitro measurement of the frequency-dependent attenuation in cancellous bone between 0.2–2.0 MHz," J Acoust Soc Am **108**, 1281–1289 (2000).
56. S. Han, J. Rho, J. Medige, and I. Ziv, "Ultrasound velocity and broadband attenuation over a wide range of bone mineral density," Osteoporosis Int **6**, 291–296 (1996).
57. C. M. Langton, S. B. Palmer, and S. W. Porter, "The measurement of broadband ultrasonic attenuation in cancellous bone," Eng Med. **13**(2), 89–91 (1984).
58. R. Strelitzki and J. A. Evans, "Diffraction and interface losses in broadband ultrasound attenuation measurements of the calcaneus," Physiol Meas **19**, 197–204 (1998).
59. K. A. Wear, "Ultrasonic attenuation in human calcaneus from 0.2 to 1.7 MHz," IEEE Trans Ultrason Ferroelectr Freq Control **48**(2), 602–608 (2001).
60. J. W. S. Rayleigh and R. B. Lindsay, *Theory of Sound* (Macmillan, London, UK, 1878).
61. P. Morse and K. Ingard, *Theoretical Acoustics* (Princetown University Press, Princetown, NJ, 1986).
62. J. C. Bamber, "Ultrasonic properties of tissue," in *Ultrasound in medicine*, F. A. Duck, A. C. Baker, and A. C. Starritt, eds. (Institute of Physics Publishing, Bristol, UK, 1998).
63. G. Haiat, A. Lhemery, F. Renaud, F. Padilla, P. Laugier, and S. Naili, "Velocity dispersion in trabecular bone: influence of multiple scattering and of absorption," J Acoust Soc Am **124**(6), 4047–4058 (2008).
64. K. A. Wear, "Frequency dependence of ultrasonic backscatter from human trabecular bone: theory and experiment," J Acoust Soc Am **106**(6), 3659–3664 (1999).